Dose-Response Characteristics of Retinal Inactivation Due to Intravitreal Injections of Tetrodotoxin in Nonhuman Primates

Randolph J. Kwaw,[1] Kevin R. Duffy,[2] Hui Meng,[1] Robert W. Jones,[2] Zainab Zehra,[1] Arnold J. Heynen,[3] Matthew S. Lawrence,[4,5] Lawrence Tychsen,[6] Mark F. Bear,[3] Laura J. Frishman,[1] Nimesh B. Patel,[1] and Vallabh E. Das[1]

[1]College of Optometry, University of Houston, Houston, Texas, United States
[2]Department of Psychology and Neuroscience, Dalhousie University, Halifax, California, United States
[3]Picower Institute for Learning and Memory, Massachusetts Institute of Technology, Cambridge, Massachusetts, United States
[4]Virscio, New Haven, Connecticut, United States
[5]St. Kitts Biomedical Research Foundation, St. Kitts, West Indies
[6]Department of Ophthalmology, Washington University at St. Louis, St. Louis, Missouri, United States

Correspondence: Vallabh Das, College of Optometry, University of Houston, 4401 Martin Luther King Blvd, Houston, TX 77204, USA; vdas@central.uh.edu.

Received: December 10, 2025
Accepted: May 13, 2026
Published: June 8, 2026

Citation: Kwaw RJ, Duffy KR, Meng H, et al. Dose-response characteristics of retinal inactivation due to intravitreal injections of tetrodotoxin in nonhuman primates. *Invest Ophthalmol Vis Sci.* 2026;67(6):12. https://doi.org/10.1167/iovs.67.6.12

Purpose. Temporary retinal inactivation of the fellow eye with intravitreal tetrodotoxin (TTX) has shown promise as a treatment strategy for deprivation amblyopia in mouse and cat models. The purpose of this study was to evaluate the duration of retinal inactivation achieved with different doses of TTX in nonhuman primates (NHPs), while also assessing functional and structural measures of vision to determine the safety of this treatment approach.

Methods. Three adult and four infant NHPs received varying doses of TTX (115–4800 ng) via intravitreal injection. Inactivation duration was assessed via contrast sensitivity function (CSF) in awake-behaving adults and visual evoked potential (VEP) responses in anesthetized infants. Safety of the TTX approach was investigated using optical coherence tomography (OCT), electroretinogram (ERG), retinal histology, and clinical evaluation of a relative afferent pupillary defect (RAPD).

Results. Inactivation duration was dose dependent. Low doses (115–230 ng) resulted in up to 4 days of inactivation. Intermediate doses (460–920 ng) extended inactivation up to 8 days, whereas the highest dose (4800 ng) eliminated VEP responses for up to 10 days. RAPD that emerged soon after the injection was absent at about the same time as CSF and VEP responses recovered to baseline. Post-inactivation assessments using OCT, ERG, or histology showed no discernible changes in retinal structure or function.

Conclusions. Intravitreal TTX at the doses examined does not cause permanent disruption of vision in primates, and the duration of retinal inactivation can be titrated by dose. The dose-response relationship provides a foundation for future studies testing the efficacy of this treatment approach in amblyopic monkeys.

Keywords: intravitreal injections, tetrodotoxin (TTX), primates, optical coherence tomography (OCT), electroretinogram (ERG), visual evoked potential (VEP), contrast sensitivity function (CSF), relative afferent pupillary defect (RAPD)

Amblyopia is a common cause of vision impairment in children and young adults, affecting 2% to 3% of the population. The condition occurs due to unequal visual input from the two eyes to the visual cortex during the critical period for visual development.[1–3] Unequal refractive error in the two eyes (anisometropia) and ocular misalignment (strabismus) are the most common amblyogenic factors. Amblyopia due to form deprivation (e.g. from unilateral congenital cataract) is less common but causes the most severe vision loss.[4] Conventional treatment for amblyopia involves addressing the underlying amblyogenic factor (e.g. cataract removal), followed by patching or penalizing the fellow eye (FE) to promote recovery of vision through the amblyopic eye (AE).[5–8] Successful recovery is more likely when patching treatment occurs within the critical period of visual development, presumably due to increased capacity for plasticity within the developing brain.[9,10] Conventional treatment approaches outside the critical period (≥7 years of age for refractive and strabismic amblyopia, and ≥10 months of age for form deprivation amblyopia) are mostly ineffective.[11–14] Further, conventional treatments face significant additional challenges, such as poor compliance, disruption of binocular input, risk of recurrence, and long treatment duration.[15–19]

The prevalence of suboptimal clinical outcomes in those with poor compliance or those treated outside of the critical period underscores the need for innovative therapy. An experimental manipulation that is effective in rodent and cat models for deprivation amblyopia is to place animals in total darkness (dark exposure) for an extended period (approximately 10 days).[20–24] However, even brief exposure to light during this period negates the beneficial effect[25] as does application at older ages.[26] Although effective and instrumental in improving our understanding of post-critical period plasticity, dark exposure for long durations is impractical as a treatment for amblyopia in children. However, the potential for dark exposure to reverse monocular deprivation amblyopia in laboratory animals has led to the idea that complete silencing of retinal activity could be an effective treatment. Thus, intraocular microinjection of tetrodotoxin (TTX) to temporarily inactivate retinal output emerged as an alternative.[27,28] Intravitreal TTX binds to voltage-gated sodium channels in the retina with high affinity and retinal activity is silenced until either new sodium channels develop or previously bound channels are released and are able to transmit action potentials upstream to the thalamus (LGN) and visual cortex.[29,30] Two days of binocular inactivation due to a single injection of TTX in the mouse and 7 days of bilateral retinal inactivation due to 2 applications of TTX in the cat was found to be effective to reverse form deprivation amblyopia in these animal models.[27] Later, it was discovered that bilateral inactivation was unnecessary and 2 days of monocular FE inactivation in the mouse and 10 days of monocular FE inactivation in the cat, delivered once every 48 hours for 4 to 5 days, was equally effective against form-deprived amblyopia.[31]

Although the data from cat/mouse work on TTX treatments is promising, the substantial variance from the human visual system underscores the need to perform studies in nonhuman primates (NHPs), as an intermediate step, before considering TTX treatment in humans. Spatial acuity is 0.5 cycles/deg in the mouse, 8 to 10 cycles/deg in cats, and up to 30 cycles/deg in monkeys and humans.[32,33] Binocularity is profoundly affected in human amblyopia but stereoacuity in the mouse and cat is much weaker than in monkeys and humans, thus elevating the importance of testing in NHPs.[34,35] Neuroanatomic differences within the LGN and V1 across species are also well-documented and include differences in total surface area, ocular dominance distributions, and neuronal characteristics.[32] In addition, the ability to reproduce human visual development disorders like strabismus, latent nystagmus, and anisometropic, or strabismic amblyopia in NHPs is well-established.[36]

In a promising pilot study involving two amblyopic infant monkeys, we showed that a small dose (115 ng) of TTX delivered via intravitreal injection into the FE resulted in temporary retinal inactivation of approximately 48 hours with partial recovery of vision in the AE as assessed by visual evoked potential (VEP) testing (Kwaw RJ et al. IOVS 2024; 65; ARVO E-Abstract 5196; Das VE et al. IOVS 2024; 65; ARVO E-Abstract 5197). Prior to initiating expanded experiments evaluating treatment in a larger cohort of amblyopic monkeys, we sought to determine whether duration of inactivation of the injected eye could be extended by changing TTX dose level, while preserving safety, that is, recovery of vision in the injected eye as determined via structural and functional testing. The goal of this study was therefore to measure a dose-response relationship for FE TTX inactivation that was deemed safe and could be used for later studies of efficacy in amblyopic monkeys.

Methods

Subjects

Data presented here are from experiments performed at two sites. Three adult rhesus monkeys (*Macaca mulatta*; M1–M3; 3–6 years of age, all male monkeys) were tested at the University of Houston, and four infant African green monkeys (*Chlorocebus sabaeus*; N1–N4; 3 months of age; 3 male and 1 female monkeys) were tested at the St. Kitts Biomedical Research Foundation (St. Kitts, West Indies). Experimental procedures were carried out in strict compliance with protocols approved by the Institutional Animal Care and Use Committees of the respective institutions.

Intravitreal Injections

TTX was delivered using intravitreal injection in the form of TTX-citrate (Tocris Biosciences CAS No: 18660-81-6) which is a water-soluble citrate salt of TTX. The TTX-citrate, originally in powder form, was reconstituted to the desired concentration by adding sterile balanced salt solution (BSS; Alcon, Fort Worth, TX, USA). For adult animals, the TTX dosage ranged between 115 and 920 ng. The volume of TTX-citrate solution injected into the vitreous chamber of the right eye was kept constant at 40 µL, and the TTX dosage was changed by altering the concentration (9–72 µM; Table 1). All infant monkeys (N1–N4) received a single injection of 4800 ng in either the left or right eye (5 µL at 3000 µM conc). The delivery method was essentially similar across all animals. The animal was sedated with an intramuscular injection of a mixture of ketamine and xylazine and topical proparacaine drops were applied to numb the eye. A sterile syringe with a 30-gauge needle was used to slowly inject the desired volume of TTX-citrate solution 1.5 to 2.0 mm posterior to the limbus. Some of the adult animals were tested at multiple doses and in these animals the injections were separated by several months to ensure that the effects of the previous injection were fully dissipated.

Assessing Visual Function

Visual function testing was different in the adult and infant animals. In the adults, we performed behavioral testing to assess the monocular contrast sensitivity function (CSF) prior to and in the days after receiving TTX injections to directly measure visual function and duration of inactivation. For CSF testing, animals were trained to behaviorally respond to a sine wave grating presented in central fixation during monocular viewing condition with the other eye occluded, as previously described.[37,38] In brief, stimuli were presented on a calibrated VPixx monitor (VPixx, version 1.5) at 80 cm from the animal's eye, at a photopic background luminance of 50 cd/m^2. Animals were refracted and viewed through corrective lenses during the testing. Animals were positively rewarded when they correctly responded, via lever release, to a 300 msec presentation of a central 4 degrees stimulus with a gaussian envelope. For each of six spatial frequencies tested (0.5, 1, 2, 4, 8, and 16 cyc/deg), a staircase method was used to determine thresholds from the last three reversals. All stimuli were presented using

Investigative Ophthalmology & Visual Science

Table 1. Summary of TTX Doses Administered (115–4800 ng) and the Corresponding Duration of Inactivation for Each Animal

Dosage	Injection Parameters, vol; Conc. of TTX-Citrate)	NHP ID	Duration of Inactivation
115 ng	40 µL; 9 µM	M1	M1: 3
230 ng	40 µL; 18 µM	M1	M1: 4
460 ng	40 µL; 36 µM	M1, M2	M1: 4; M2: 6
920 ng	40 µL; 72 µM	M1, M2, M3	M1: 7; M2: 8; M3: 7
4800 ng	5 µL; 3000 µM	N1, N2, N3, N4	N1–N4: 10

M1 to M3 are adults and N1 to N4 are infants. For doses between 115 ng and 920 ng, duration of inactivation was determined based on the absence of responses during contrast sensitivity function (CSF) testing, whereas, for the 4800 ng dose, inactivation was assessed by the absence of visual evoked potential (VEP) responses.

Psychtoolbox,[39] and the behavioral system controlled using programs written in Matlab (Mathworks, Natick, MA, USA).

The learning required for behavioral testing is not possible in infant animals; therefore, VEP measurements during monocular viewing were used to test visual cortical responsivity to the displayed stimulus, which served as a proxy to functional vision.[40–43] After sedation with a mixture of ketamine and xylazine, animals were prepared for VEP testing by shaving the head to ensure good contact with 3 reusable 10 mm gold cup electrodes that were affixed to the scalp with conductive gel (neurodiagnostic electrode paste, Ten20). One electrode was placed on the forehead as a reference electrode and 2 electrodes were placed 1 to 4 mm laterally to the Oz on either side to record responses from each visual cortex hemisphere. Visual stimuli were generated using custom MATLAB software with the Psychophysics Toolbox extension. The stimuli consisted of full-contrast square wave gratings that phase reversed with a 4 hertz (Hz) reversal frequency. Blocks of varying spatial frequencies (0.25, 0.5, 1, 2, and 4 cyc/deg) were presented in pseudo-random order for 20 seconds each, interspersed with an 8-second gray screen interstimulus interval. Each eye was tested individually with the other eye occluded. EEG signals were recorded with Open-Ephys hardware and software, and data were analyzed offline using MATLAB custom software. The data analysis consisted of performing a Fourier transform of the raw electroencephalogram (EEG) waveform for each spatial frequency and calculating the sum of the amplitude spectrum at the stimulus fundamental frequency and six additional harmonics. Data from four blocks of visual presentations were averaged to yield an estimate of VEP amplitude response at each spatial frequency.

Assessing Retinal Structure and Function

Although tests such as the CSF or the VEP provide an indication of inactivation duration and visual function recovery in the injected eye, assessment of retinal integrity is critical to assess the safety of intravitreal TTX administration. Retinal structure and function before and 3 to 5 months after TTX injections were investigated using OCT and ERG methods in the adult animals that received the highest dose of 920 ng of TTX.[44,45] For these measurements, the adult monkeys were sedated with a mixture of ketamine (20–25 mg/kg/hr) and xylazine (0.8–0.9 mg/kg/hr), with a subcutaneous injection of atropine sulfate (0.04 mg/kg). Heart rate and blood oxygen were monitored with a pulse oximeter (model 9847V; Nonin Medical, Inc., Plymouth, MN, USA). Body temperature was maintained between 36.5°C and 38°C with a heating pad. Optical coherence tomography (OCT) imaging consisted of a high-resolution wide-field 55 degrees × 45 degrees raster scan with 9 frame averaging, and isotropic 20 degrees × 20 degrees OCT angiography (OCTA) scans centered on the optic nerve head and macula (Spectralis OCT, Heidelberg Engineering, Heidelberg, Germany). Raw images were analyzed by programs in MATLAB to assess optic nerve head morphology, circumpapillary retinal nerve fiber layer thickness, ganglion cell inner plexiform layer thickness, and retinal vascular density, before and after TTX application.

Rhesus monkeys have retinas that are sufficiently similar structurally and functionally to those of humans that ERG tests of rod and cone-driven retinal function that are used in humans are appropriate for testing monkeys.[46] At the time of testing, pupils were dilated with topical tropicamide (1%) and phenylephrine 2.5%. ERGs were recorded with Dawson-Trick-Litzkow (DTL) electrodes that were moistened with lubricant (Refresh Celluvisc; Allergan). Electrodes were positioned across the center of the cornea, under a nominally plano corneal contact lens on each eye. The non-stimulated eye was covered with a black eye patch and cloth. A metal hypodermic needle in the skin of the upper back served as the ground electrode. Recordings were amplified and filtered (DC-300 Hz). We recorded light-adapted full-field flash ERGs using an Espion E3 Ganzfeld stimulator system (Espion ColorDome; Diagnosys LLC, Lowell, MA, USA) to assess photoreceptor (a-wave), bipolar cell (b-wave), and retinal ganglion cell (RGC) function (photopic negative response [PhNR]).[47,48] ERG responses were recorded to brief (<5 ms) International Society for Clinical Electrophysiology of Vision (ISCEV) standard white flashes of 2.84 cd.s.m-2[47] and to brief red flashes, (<5 ms; λmax = 650 nm, 2.84 cd.s.m-2) on a rod saturating blue background (λmax = 462 nm, 10 photopic cd/m^2) to facilitate measurement of the PhNR.[48] Responses were averaged over 20 trials. Analyses, conducted using a custom MATLAB program, included measurement of the amplitude below baseline (0 mV) of a-wave, b-wave, and PhNR at the time after the stimulus flash for which each response was maximal, that is, the implicit time.[47] These values for the injected eye pre- and post-TTX application are reported in the Results section for responses to the red flash stimuli.

Retinal Histology

Anatomic analysis of the retinas was performed on the four infant monkeys that received the highest dose of intravitreal TTX (i.e. 4800 ng). Ten weeks after TTX injection, the animals were sedated with an intramuscular injection of ketamine/xylazine and then were euthanized with intravenous administration of sodium pentobarbital (100 mg/kg).

Tissues were flushed by transcardial perfusion with PBS (500 mL), followed by perfusion fixation with 4% paraformaldehyde dissolved in PBS (500 mL). Globes were further fixed in Davidson's solution for 24 hours, then transferred to PBS with 0.05% sodium azide for storage and shipment. Histological processing was performed by Virscio Inc. (New Haven, CT, USA). Globes were trimmed horizontally into three sections prior to processing. Tissues were dehydrated in alcohol, cleared in xylene, and then infiltrated with paraffin in preparation for sectioning. Tissue sections were cut at 5 mm, then were processed for standard hematoxylin and eosin (H&E) staining. Slides were imaged using a P150 slide scanner (3DHistotech, Budapest, Hungary) fitted with a 20 × objective. Quantification of cell density and soma size was performed on the ganglion cell layer (GCL), the inner nuclear layer (INL), and the outer nuclear layer (ONL) from the retinas of control eyes and those subjected to intravitreal TTX.[49] The automated cell detection feature in QuPath software was used to count cells and measure soma areas. For each animal, retinal cells were selected for quantification using a threshold classifier that was configured to detect the outer boundary of cell somata. A separate classifier was optimized for each of the retinal layers quantified. These classifiers enabled automated cell detection and measurement, and these parameters were applied equally to all sections from each monkey examined. This quantification approach permitted sampling from a large region of the retina (approximate total area per retina = 0.65 mm^2) that spanned the fovea as well as the periphery. Cell density was calculated for each layer by dividing the obtained cell count by the area of the sample region.

Clinical Evaluation

For all animals, including the infant monkeys, a qualitative evaluation of a relative afferent pupillary defect (RAPD) that emerged after TTX injection was conducted. In addition, for the adult monkeys, change in intraocular pressure (IOP) following the intravitreal injection was monitored in the minutes after the injection with an iCare TONOVET rebound tonometer.[50]

Results

Dose-Dependency of Inactivation Following Intravitreal Injections of TTX

Intravitreal TTX doses ranging from 115 to 4800 ng were injected into 7 monkeys, and the duration of inactivation was measured either via behavioral CSF estimation in adults or via VEP testing in infants. In adult animals, we began with the lowest dose (115 ng) and progressively increased it, roughly doubling the dose with each subsequent injection, up to 920 ng. Panels of Figure 1 show results of contrast sensitivity testing in one adult monkey (M1). At 115 ng (see Fig. 1A), CSF was immeasurable a day post-TTX, partially recovered to 75% on day 2, and was fully recovered by day 3. At 230 ng (see Fig. 1B), CSF was immeasurable for 2 days, showed partial recovery to 53% by day 3, and was fully recovered to baseline by day 4. At 460 ng (see Fig. 1C), CSF was immeasurable for 2 days, partially recovered to 80% by day 3 and fully recovered by day 4. At 920 ng (see Fig. 1D), CSF was immeasurable for 4 days, partially recovered to 29% by day 5, and fully recovered by day 7. A second animal (M2)

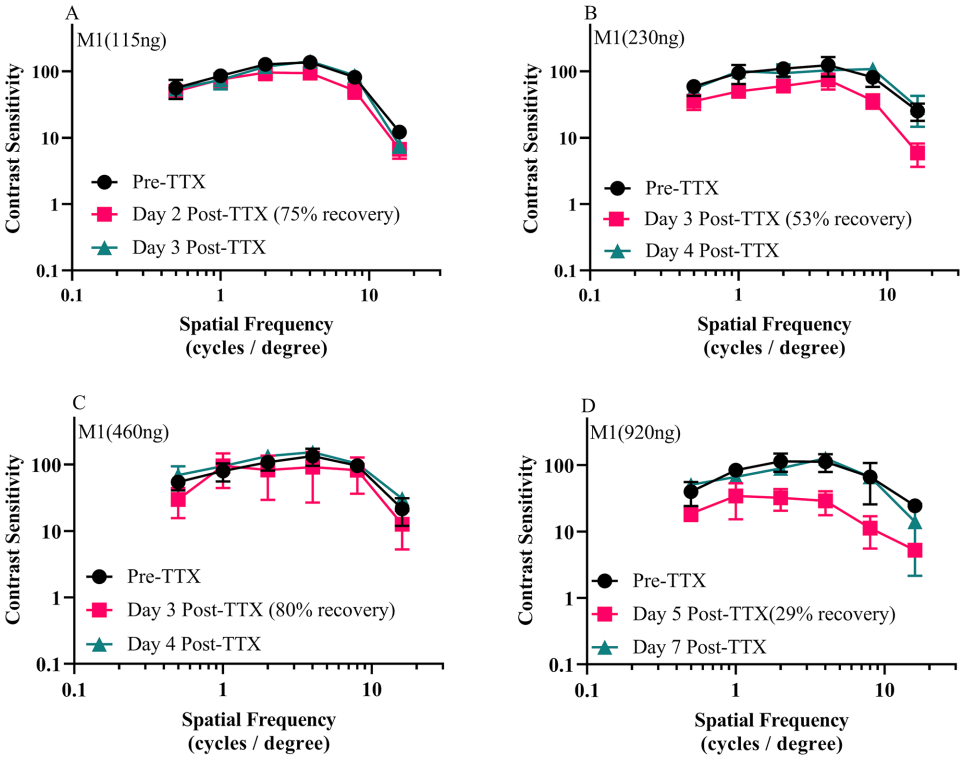

Figure 1. Behavioral contrast sensitivity function (CSF) responses of animal M1 before and after intravitreal injections of different amounts (panels **A–D**) of TTX. *Black* = baseline CSF before injections; *magenta* = post-TTX CSF on the first day that it was measurable; *teal* = post-TTX CSF on the first day that it returned to baseline. Error bars are SEM.

Investigative Ophthalmology & Visual Science

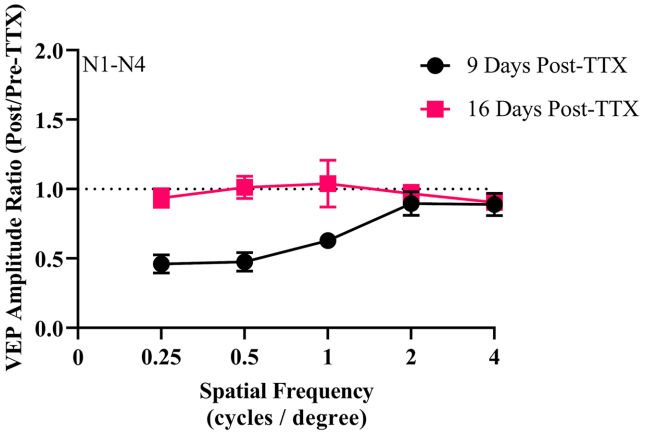

Figure 2. Ratio of visual evoked potential (VEP) responses after TTX injection to VEP responses before TTX injections in infant animals ($n = 4$). A ratio of 1.0 would indicate complete recovery of vision as measured by the VEP response. Error bars are SEM.

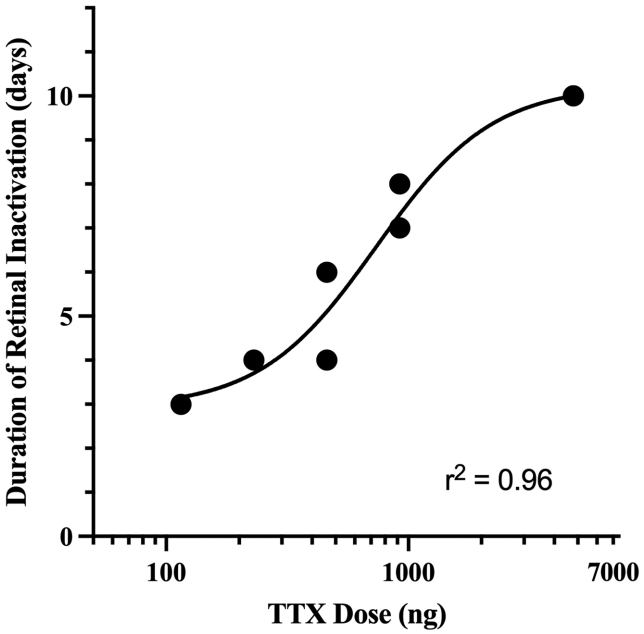

Figure 3. Summary plot of the duration of inactivation across doses ranging from 115 ng to 4800 ng in adult ($n = 3$) and infant animals ($n = 4$). Data are plotted based on data in Table 1 and the following fit equation available in GraphPad Prism: Duration = Bottom + (Top-Bottom)/(1+(EC50/Dose)^HillSlope). In this equation, "Bottom," "Top," "EC50," and "HillSlope" are free variables and represent the parameters of the sigmoidal curve fit.

also received the 460 ng injection and 2 additional animals (M2 and M3) also received the highest dose of 920 ng and each of these experiments yielded comparable durations of retinal inactivation to respective doses for M1. Table 1 shows a summary of the different doses attempted and the days of inactivation achieved at each dose for all the animals tested.

We also delivered TTX injections to four infant African green monkeys that each received a single injection of 4800 ng of TTX. In these animals, recovery of function was estimated by measuring VEP responses before and in the days after the injection. Figure 2 plots the ratio of pre- and post-TTX VEP amplitudes at each of the spatial frequencies tested and shows that average VEP responses across all spatial frequencies tested were partially recovered to 56% by day 9 and fully recovered when next tested on day 16. Although we did not get the opportunity to measure VEP responses between day 9 and day 16 due to limitations in the number of sedations possible in infant animals, we estimate that full recovery occurred on day 10 or day 11. Our estimate of projected full recovery in the infants was based on observation that, in all adult animals and at all doses tested, full recovery was achieved less than 48 hours after partial recovery was first detected (see Fig. 1 for example in M1). Note that VEP response was tested 3 times in the first 8 days and was not measurable through the injected eye.

The cumulative data from the adult and infant animals are plotted in Figure 3 and suggests TTX dose-dependent duration of retinal inactivation in the injected eye. Data were fit in GraphPad Prism version 10.5 using the dose-response family of nonlinear regression curves. In the context of a pharmacological dose-response, where the dose is the amount of TTX and the response is the duration of retinal inactivation, the dose required for 50% of maximal response (retinal inactivation in this case) was estimated to be 736 ng (66% of maximal response: approximately 1000 ng and 80% of maximal response: approximately 1500 ng).

Assessing the Safety of Intravitreal TTX Injections

No extraocular or intraocular clinical signs of TTX treatment (e.g. endophthalmitis) were observed in any animal. In all animals, an RAPD emerged soon after delivery of the TTX injection and pupillary response was assessed for recovery. Our main observation was that the presence of RAPD and the duration over which CSF or VEP could not be measured, overlapped. Further, RAPD was absent at approximately the same time that the CSF or VEP measures of visual function had recovered. Hence, RAPD and subsequent recovery can potentially serve as an indirect measure of visual function recovery in the injected eye. In addition, the changes in IOP following delivery of a 40 µL volume of solution in adult monkeys was measured (Fig. 4). Prior to injection, the average IOP was 14 millimeters of mercury (mm Hg), which increased to 45 mm Hg immediately following the intravitreal injection and returned close to baseline (20 mm Hg) in approximately 5 minutes.

We also performed OCT/OCTA and ERG testing in the adult animals (M1–M3) that received the 920 ng of TTX to assess for structural loss, and physiological recovery of the retina from the TTX injections. Figure 5 and Table 2 show the results from OCT/OCTA imaging before and after injections. Figure 5A shows pre- and post-TTX B-scan sections in animal M2 showing no gross differences in retinal anatomy of optic nerve head morphology. Widefield thickness maps (55 degrees × 45 degrees scans), generated from 217 B-scans with 9 frame averaging, showed no differences in either retinal nerve fiber layer (RNFL) thickness or ganglion cell inner plexiform layer (GCIPL) thickness (see Figs. 5C, 5D, respectively). Circumpapillary RNFL and macula GCIPL thickness in the animals pre- and post-injection is provided in Table 2 and were not significantly different (Wilcoxon matched-pairs signed-rank test; $P > 0.05$). Because the sample size is small, statistical tests are of low power, and it is appropriate to compare the changes in RNFL and GCIPL thickness to normative measures of test-retest variability described in the literature. None of the thickness measurements in the

Investigative Ophthalmology & Visual Science

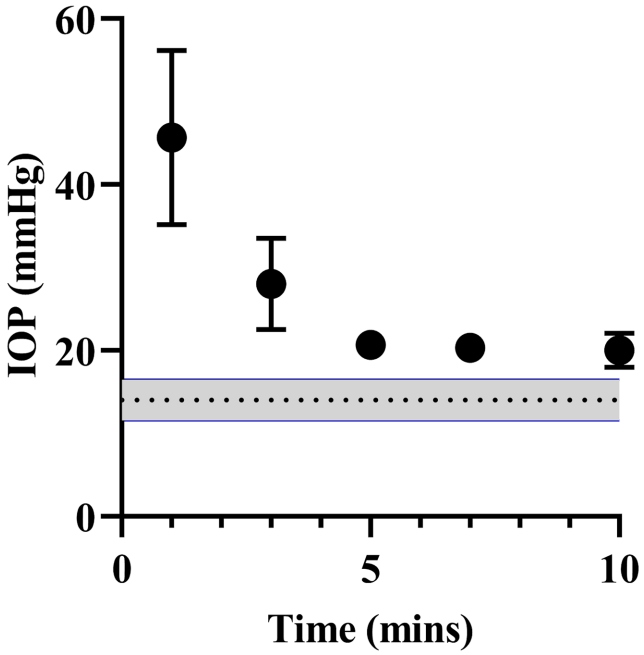

Figure 4. Average intraocular pressure (IOP) measured immediately after a 920 ng injection in adult animals ($n = 3$). Time zero indicates the time at which the injection needle was retracted from the eye. The *shaded horizontal band*, centered on the *dotted reference line*, represents the IOP range in these animals prior to injection. Error bars are SEM.

current study showed changes greater than 4 to 7 µm and 2 to 3 µm, which is within the bounds of test-retest variability for RNFL and GCIPL, respectively.[51–55] In addition, OCTA (see Fig. 5B) centered on the optic nerve and macula showed no changes in major retinal vasculature (MRV), the radial peripapillary capillaries (RPCs), and the superficial vascular complex (SVC). In summary, there was no indication that retinal structure was affected by the highest dose of TTX that was tested in the adult animals.

Table 2. Global Retinal Nerve Fiber Layer (RNFL) and Ganglion Cell Inner Plexiform Layer (GCIPL) Thickness for Monkeys M1 to M3 Before and 3 Months After Injection With 920 ng of TTX

NHP ID	RNFL Pre, µm	RNFL Post, µm	GCIPL Pre, µm	GCIPL Post, µm
M1	133	138	76	78
M2	116	116	70	71
M3	129	130	72	75

To assess the long-term effect of TTX injections on retinal function, we measured light-adapted ERG responses in the injected eye of three adult animals (M1, M2, and M3) before, and again 3 to 5 months after the injection (Figs. 6A–C). Table 3 shows amplitudes and implicit times of responses to brief red flashes for the light-adapted ERG a-wave (reflecting photoreceptor and off bipolar cell activity), b-wave (mainly on bipolar cell activity), and the PhNR (RGC activity).[46] The amplitude and implicit times did not show significant differences in responses before and post-TTX injections (Wilcoxon matched-pairs signed-rank test; $P > 0.05$). As with the OCT data, due to small sample size concerns, we also considered the ERG data within the framework of test-retest variability. Fortune and colleagues performed a study in 23 NHPs and reported that a-wave amplitude would have to change by 45.8%, b-wave amplitude would have to change by 63.3% and PhNR amplitude would have to change by 63.0% in order for intersession differences to be considered significant.[56] Pre- and Post-TTX percentage a-wave and b-wave amplitude differences in all animals were well within these bounds (a-wave = 0.87%–18.94% and b-wave = −5.03% to 15.9%). PhNR amplitude differences in M1 and M3 were also within the bounds (M1 = 46.18% and M3 = 18.33%). Only in animal M2, was the

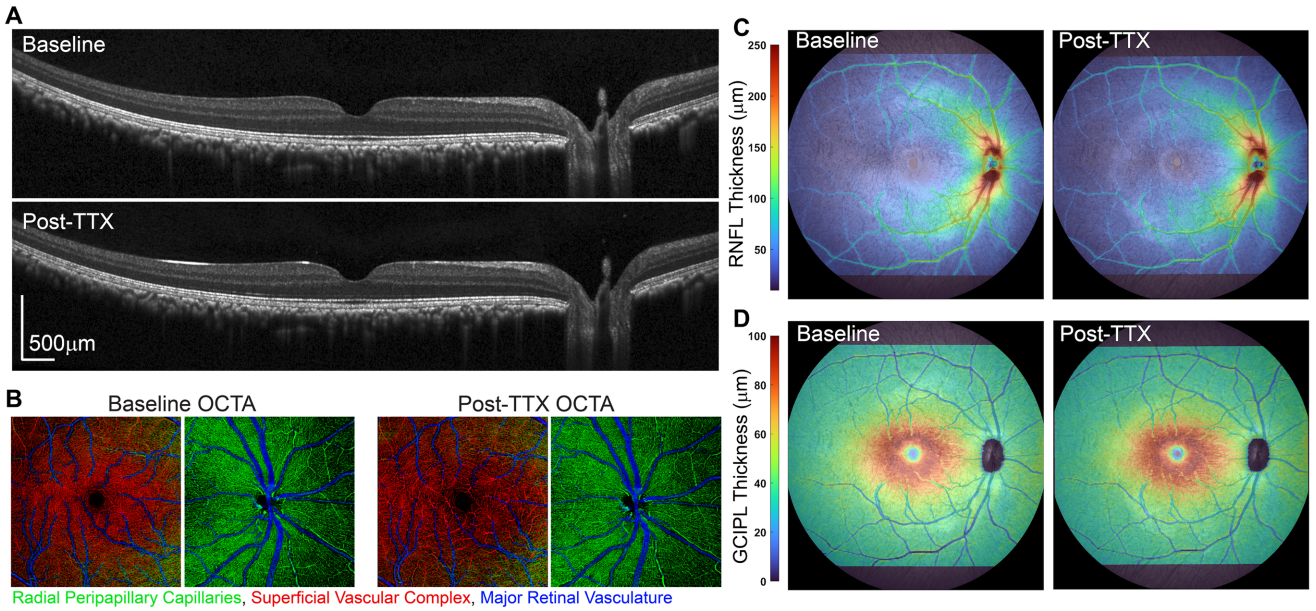

Figure 5. Panel (**A**) OCT B-scans in M2 before and 3 months after TTX. Panel (**B**) OCTA showing radial peripappilary capillaries (*green*), superficial vascular complex (*red*), and major retinal vascualature (*blue*) before and after TTX. Panels (**C, D**) Widefield thickness maps of retinal nerve fiber layer (RNFL) and ganglion cell inner plexiform layer (GCIPL) before and after TTX.

Investigative Ophthalmology & Visual Science

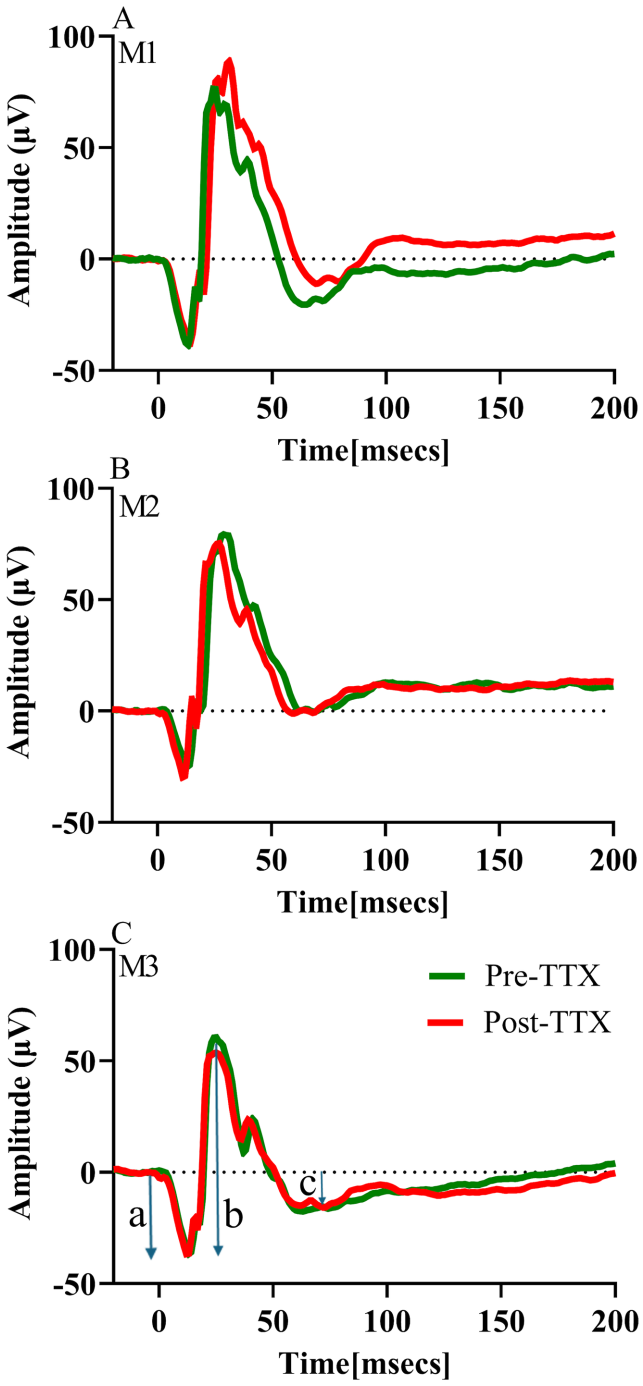

Figure 6. Electroretinogram (ERG) responses of the injected eye before and 3 to 5 months after 920 ng TTX injection for animals M1 to M3. The initial negative deflection corresponds to the a-wave (**A**), reflecting photoreceptor activity, followed by the positive b-wave (**B**), which represents bipolar cell responses. The later, smaller negative component is the photopic negative response (PhNR) (**C**), associated with RGC function.

difference in pre- and post-TTX PhNR amplitude outside the benchmark value reported by Fortune and colleagues. Note, however, that in this animal, the PhNR amplitude below baseline was negligible in the pre-TTX record, which occurs in some subjects. The post-TTX response was also present, and in fact larger than the pre-TTX response, but was still very small. These small responses would distort the assessment of significant difference.

Sections of retina from infant animals in this study that received the highest dose of TTX (N1–N4) showed no qualitative differences in H&E staining between the inactivated and fellow control eyes (Fig. 7A). Quantification of cell density was measured separately across the GCL, INL, and ONL (Fig. 7B) from cross sections of the retina that included the fovea, periphery, as well as the optic nerve. Average densities calculated from the control and inactivated retinas were comparable across the layers sampled (Table 4). Wilcoxon matched-pairs signed rank test performed separately for each layer revealed no statistically significant differences in cell density ($P > 0.05$). We also quantified the cross-sectional area of cell somata across retinal layers. The average soma area measured from the control and inactivated retina were very similar across all layers examined (see Table 4). A Wilcoxon matched-pairs signed rank test revealed no statistical difference between the control and inactivated retina for the layers examined ($P > 0.05$). These results indicate that at the highest TTX dose administered in this study, there was no evidence of retinal histopathology in the inactivated eye.

Discussion

Conventional treatments for amblyopia are burdensome and often ineffective. Therefore, alternative effective treatments are needed.[8] Monocular retinal inactivation with TTX could be a transformative treatment that effectively restores vision in the amblyopic eye and rebalances ocular dominance, even beyond the critical period.[27,31] To translate this treatment to humans, it is necessary to test NHPs, whose spatial acuity, binocularity, visuomotor behavior, ocular dominance distribution, and neuronal characteristics closely resemble those of humans.[32,35] In this study, we have determined a dose-response relationship (between TTX amounts and the duration of retinal inactivation) at intravitreal doses that are safe and optimize the duration of inactivation.

A clear dose-response relationship was evident in our data. Lower doses (115 ng and 230 ng) produced shorter durations of inactivation, with recovery to baseline within 3 to 4 days. Intermediate doses (460–920 ng) extended the duration of inactivation to 6 to 7 days, with partial recovery observed before recovering to baseline. The highest tested dose (4800 ng in infant monkeys) prolonged inactivation, with complete absence of VEP responses for 8 days, partial recovery on day 9, and projected full recovery by days 10 or 11. The dose-response relationship yielded half maximal effective dose of approximately 700 ng and doses of 1000 to 1500 ng TTX were in the 66% to 80% range of maximal duration of inactivation. From these data, a dose of 1000 to 1500 ng of TTX could represent the smallest dose that yields maximal impact in terms of days of retinal inactivation. This insight could be of critical importance for circumstances in which long durations of TTX-induced FE inactivation are needed to produce optimal recovery of vision in the AE.

Why does a higher dose of TTX result in longer inactivation and why does this dose-response relationship saturate? It appears that TTX binds to sodium channels with a 1:1 relationship as in one molecule of TTX binds with one sodium channel.[57] In the dose range of 115 to 920 ng, there are approximately 2×10^{14} to 8×10^{14} molecules of TTX that are available in the vitreous chamber upon injection. Considering that there are approximately 1.5×10^{6}

Investigative Ophthalmology & Visual Science

Table 3. Summary of the Pre- and Post-TTX Photopic ERG Responses in Adult Animals M1 to M3

	a-Wave, Amp (μV) (IT (ms))		b-Wave, Amp (μV) (IT (ms))		PhNR, Amp (μV) (IT (ms))	
NHP ID	**Pre-TTX**	**Post-TTX**	**Pre-TTX**	**Post-TTX**	**Pre-TTX**	**Post-TTX**
M1	−38.51	−37.56	76.48	88.65	−20.46	−11.01
	13	14	24	31	65	69
M2	−24.97	−29.7	79.36	75.37	−0.18	−1.09
	13	11	29	27	69	59
M3	−36.59	−36.91	60.53	53.86	−17.51	−14.3
	13	12	25	25	63	71

Amplitudes (Amp, μV) and Implicit times (IT, ms) are reported for the a-wave, b-wave, and photopic negative response (PhNR).

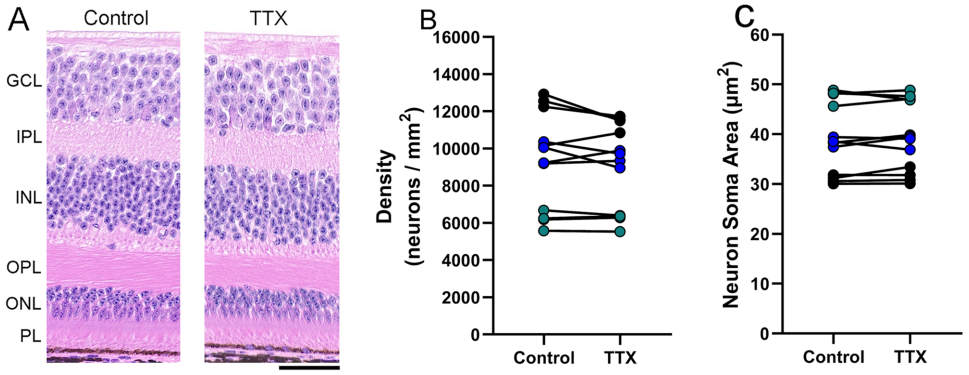

Figure 7. Quantification of retinal cell density and soma size following monocular intravitreal injection of TTX in infant monkeys ($n = 4$). Qualitative assessment of retinal sections stained for H&E revealed no obvious laminar differences between the control and inactivated eyes (**A**). Separate quantification of cell density and soma area across retinal layers (Panels **B** and **C**; GCL - *teal*, INL - *black*, and ONL - *blue*) revealed comparable measurements between the retinas that were not statistically different. *Scale bar* = 50 microns.

Table 4. Summary of Cell Density Measurements (Neurons/mm^2) and Cross-Sectional Soma Area Measurements (mm^2) From the Layers Sampled From the Control and TTX-Inactivated Retinae of Infant Monkeys N1 to N4

	Cell Density		Cell Area	
	Control, Mean ± SD	**TTX, Mean ± SD**	**Control, Mean ± SD**	**TTX, Mean ± SD**
GCL	6,169 ± 454	6,146 ± 414	47.71 ± 1.42	47.63 ± 0.87
INL	11,972 ± 1245	11,413 ± 389	30.93 ± 0.76	31.54 ± 1.43
ONL	9,711 ± 590	9,480 ± 416	38.43 ± 0.80	38.82 ± 1.31

GCL, ganglion cell layer; INL, inner nuclear layer; ONL, outer nuclear layer.

RGCs in the macaque retina,[58,59] the number of molecules of TTX available per ganglion cell is approximately 1×10^8 to 5×10^8. Although the number of sodium channels per ganglion cell is unknown, it is safe to assume that it would be orders of magnitude less than the molecules of free TTX that are available. Therefore, even allowing for binding of free TTX to other ocular structures in the vicinity, such as the iris and ciliary body, it is likely that the reason for increased duration of inactivation with larger dose is due to initially unbound TTX in the vitreous that continues to bind to newly formed voltage-gated sodium channels (or to channels that were previously bound and were subsequently released) in the RGCs. The availability of free-TTX is, however, also limited by outflow from the vitreous via the choroid and retinal pigment epithelium, potentially explaining the saturation of the dose-response curve.[60] In assessing the dose-response relationship, it is reasonable to question whether data from infant and adults of two different species of NHPs may be combined. We do not believe that species differences are a consideration because structure of the retina, including numbers of ganglion cells and ERG responses, are comparable between the African green monkey and the rhesus monkey.[61,62] With respect to age, RGC number is established prenatally and does not increase after birth. Whereas prenatal developmental events, such as retinal waves, are likely influenced by channel development,[63] it seems that RGC sodium channel physiology is predominantly mature by birth or soon after.[64] A study in rats showed that 90% of sodium channels with affinity to saxitoxin (a neurotoxin similar to TTX) emerged by postnatal day 21 and that the sodium channels were concentrated in the axon initial segment as in the adult.[65] The vitreous in the infant is gel-like and undergoes liquefaction as aging proceeds.[66] However, in the rhesus monkey, liquid pockets were infrequently observed in animals less than 6 years of age[67] and therefore may not be a factor in influencing outflow of TTX in our adult sample. There may indeed be other factors influencing the rate of drug metabolism that are different in adults and infants, and further confirmation of duration of inactivation will be sought when conducting

Investigative Ophthalmology & Visual Science

studies evaluating the efficacy of TTX treatments for amblyopia in infants and in adults. The current data provide us a framework to guide efficacy studies in amblyopic animals.

A critical consideration prior to commencing further efficacy studies in amblyopic monkeys is whether the chosen TTX dose is safe, that is, does the injected eye recover its function? This is paramount in amblyopia therapy because the eye that will be injected is the "good" non-amblyopic eye. Safety was assessed across functional and structural measures in the monkeys examined. The presence and absence of RAPD approximately paralleled loss and recovery of visual function (CSF), supporting the reliability of this marker as a clinical indicator of inactivation. More importantly, in all animals, the CSF (VEP in the case of infant animals) recovered to baseline values suggesting full functional recovery of vision of the injected eye. OCT imaging revealed no structural or vascular changes in the retina or optic nerve head when measured at 3 months post-TTX, well after the TTX effect dissipated. RNFL and GCIPL thickness measurements remained within the test-retest reproducibility reported by several studies in both humans and NHPs. ERG recordings also demonstrate preserved photoreceptor, bipolar cell, and RGC function once the effect of TTX wore off. One of the animals in the study, M2, showed a lack of a measurable PhNR below baseline, both pre- and post-injection, which potentially makes it difficult to assess long-term effect of TTX on ganglion cell function in this animal. Low amplitude PhNR are sometimes observed in NHPs (see Fig. 4 in Ref. 30) and this may be due to physiological variability. Despite the lack of PhNR, the overall ERG pattern in this animal is virtually identical pre- and post-injection suggesting that the TTX did not disrupt retinal function in the long-term.

Although the infant monkeys that received the highest dose (4800 ng) were not assessed for safety using ERG or OCT, post-TTX VEP amplitudes recovered to pre-TTX baseline between day 9 and day 16, which was in-sync with absence of RAPD. Further, histological evaluation of the retina did not show any evidence of retinal histopathology due to TTX injections. Note that previous studies in cats, monkeys, and tree shrews also reported no evidence of gross ocular abnormalities following monocular intravitreal administration of TTX.[68–70] No obvious abnormalities were observed even in monkeys administered repeated high doses of TTX (19,000 ng in 10 mL volume) and for inactivation durations that lasted beyond a month.[69] More recently, DiCostanzo and colleagues[71] performed a histological evaluation of retinal layers and optic nerve in 6 cats treated with up to 9500 ng of TTX and found no differences in GCL density or soma sizes between treated and control eyes and also no difference in neurofilament labeling of treated and control optic nerves. Together, the results from both the infant and adult monkeys and other species indicate that intravitreal TTX is well-tolerated at the doses tested, with no long-term adverse effects on retinal structure or physiology.

Systemic TTX levels, in the blood or urine, for example, were not directly measured in this study. However, there was no evidence suggesting that TTX escaped from the injected eye into the systemic circulation, such as changes in behavior, respiration, feeding, or general activity. Studies in amblyopic mice and cats also have not reported any systemic effects.[27,31] Stryker and Harris[28] administered much larger TTX doses (up to 80,000 ng) in kittens either intravitreally or systemically over a 5-week period and did not report adverse behavioral effects. In a clinical trial on cancer pain management, 60,000 ng of TTX was administered subcutaneously daily for 4 days in 165 patients with minimal adverse events noted.[72] Our proposed dosage of approximately 1000 ng is roughly 60-fold lower and is therefore unlikely to produce systemic complications. Although no visual or ocular complications were observed in this study, it should be noted that intravitreal injections may present some intrinsic risks unrelated to the active ingredient, such as causing endophthalmitis or brief ocular hypertension that are of very low probability but can have devastating consequences.[73,74] Strict sterile techniques and careful post-injection monitoring can minimize risk and subsequent complications associated with intravitreal injection. With the volume that we chose of 40 µL, transient increase in IOP normalized towards baseline in approximately 5 minutes. Clinically, intravitreal injections are now accepted as a routine and safe route of administration for the management of neovascular disease.

In summary, our results provide evidence that monocular retinal inactivation using TTX is effective and safe in NHPs. The duration of inactivation can be titrated by dose, laying the foundation for future treatment of amblyopic monkeys. Those studies will determine whether the cortical reorganization and visual recovery observed in amblyopic mice and cats[31] can be replicated in primates. If successful, monocular retinal inactivation may represent a promising therapeutic avenue for treating amblyopia in humans, particularly in individuals who are beyond the critical period and for whom conventional treatments are largely ineffective.

Acknowledgments

The authors thank Merissa O'Connor, Richard Bouffard, Igor Mikaelian, Gabrielle Myers, and Vernard Woodley of the St. Kitts Biomedical Research Foundation for help with animal care and testing of the African green monkeys in the project.

Supported by the NIH under Grant R01-EY026568 (PI: Das), and UHCO Core Grant P30 EY07551 and CIHR 180287 (PI: Duffy).

Disclosure: **R.J. Kwaw**, None; **K.R. Duffy**, Reboot Vision LLC (F); **H. Meng**, None; **R.W. Jones**, None; **Z. Zehra**, None; **A.J. Heynen**, Reboot Vision LLC (F); **M.S. Lawrence**, Virscio Inc. (O); **L. Tychsen**, Reboot Vision LLC (F). This financial interest has been disclosed to University of Houston and appropriate steps have been taken to address any potential conflicts of interest; **M.F. Bear**, Reboot Vision LLC (F); **L.J. Frishman**, None; **N.B. Patel**, None; **V.E. Das**, Reboot Vision LLC (F)

References

1. Friedman DS, Repka MX, Katz J, et al. Prevalence of amblyopia and strabismus in white and African American children aged 6 through 71 months the baltimore pediatric eye disease study. *Ophthalmology*. 2009;116(11):2128–2134.
2. Multi-ethnic Pediatric Eye Disease Study Group. Prevalence of amblyopia and strabismus in African American and hispanic children ages 6 to 72 months: the multi-ethnic pediatric eye disease study. *Ophthalmology*. 2008;115(7):1229–1236.
3. Simons K. Amblyopia characterization, treatment, and prophylaxis. *Surv Ophthalmol*. 2005;50(2):123–166.
4. Antonio-Santos A, Vedula SS, Hatt SR, Powell C. Occlusion for stimulus deprivation amblyopia. *Cochrane Database Syst Rev*. 2020;3(3):CD005136.
5. Writing Committee for the Pediatric Eye Disease Investigator Group, Cotter SA, Foster NC, et al. Optical treatment of stra-

bismic and combined strabismic-anisometropic amblyopia. *Ophthalmology*. 2012;119(1):150–158.
6. Pediatric Eye Disease Investigator Group. A randomized trial of atropine vs patching for treatment of moderate amblyopia in children. *Arch Ophthalmol*. 2002;120(3):268–278.
7. Wallace DK, Repka MX, Lee KA, et al. Amblyopia Preferred Practice Pattern. *Ophthalmology*. 2018;125(1):P105–P142.
8. Meier K, Tarczy-Hornoch K. Recent treatment advances in amblyopia. *Annu Rev Vis Sci*. 2022;8:323–343.
9. Hensch TK, Quinlan EM. Critical periods in amblyopia. *Vis Neurosci*. 2018;35:E014.
10. Hubel DH, Wiesel TN. The period of susceptibility to the physiological effects of unilateral eye closure in kittens. *J Physiol*. 1970;206(2):419–436.
11. Holmes JM, Levi DM. Treatment of amblyopia as a function of age. *Vis Neurosci*. 2018;35:E015.
12. Birch EE, Duffy KR. Leveraging neural plasticity for the treatment of amblyopia. *Surv Ophthalmol*. 2024;69(5):818–832.
13. Birch EE, Stager DR. The critical period for surgical treatment of dense congenital unilateral cataract. *Invest Ophthalmol Vis Sci*. 1996;37(8):1532–1538.
14. Pfeifer W. Managing pediatric cataract patients: amblyopia treatment and binocularity outcomes. *J Binocul Vis Ocul Motil*. 2023;73(4):109–114.
15. Awan M, Proudlock FA, Grosvenor D, Choudhuri I, Sarvananthan N, Gottlob I. An audit of the outcome of amblyopia treatment: a retrospective analysis of 322 children. *Br J Ophthalmol*. 2010;94(8):1007–1011.
16. Birch EE. Amblyopia and binocular vision. *Prog Retin Eye Res*. 2013;33:67–84.
17. Hussein MA, Coats DK, Muthialu A, Cohen E, Paysse EA. Risk factors for treatment failure of anisometropic amblyopia. *J AAPOS*. 2004;8(5):429–434.
18. Stewart CE, Moseley MJ, Stephens DA, Fielder AR. Treatment dose-response in amblyopia therapy: the Monitored Occlusion Treatment of Amblyopia Study (MOTAS). *Invest Ophthalmol Vis Sci*. 2004;45(9):3048–3054.
19. Birch EE, Kelly KR. Amblyopia and the whole child. *Prog Retin Eye Res*. 2023;93:101168.
20. Duffy KR, Mitchell DE. Darkness alters maturation of visual cortex and promotes fast recovery from monocular deprivation. *Curr Biol*. 2013;23(5):382–386.
21. He HY, Ray B, Dennis K, Quinlan EM. Experience-dependent recovery of vision following chronic deprivation amblyopia. *Nat Neurosci*. 2007;10(9):1134–1136.
22. Lingley AJ, Mitchell DE, Crowder NA, Duffy KR. Modification of peak plasticity induced by brief dark exposure. *Neural Plast*. 2019;2019(1):3198285.
23. Montey KL, Eaton NC, Quinlan EM. Repetitive visual stimulation enhances recovery from severe amblyopia. *Learn Mem*. 2013;20(6):311–317.
24. Montey KL, Quinlan EM. Recovery from chronic monocular deprivation following reactivation of thalamocortical plasticity by dark exposure. *Nat Commun*. 2011;2:317.
25. Mitchell DE, MacNeill K, Crowder NA, Holman K, Duffy KR. Recovery of visual functions in amblyopic animals following brief exposure to total darkness. *J Physiol*. 2016;594(1):149–167.
26. Holman KD, Duffy KR, Mitchell DE. Short periods of darkness fail to restore visual or neural plasticity in adult cats. *Vis Neurosci*. 2018;35:E002.
27. Fong MF, Mitchell DE, Duffy KR, Bear MF. Rapid recovery from the effects of early monocular deprivation is enabled by temporary inactivation of the retinas. *Proc Natl Acad Sci USA*. 2016;113(49):14139–14144.
28. Stryker MP, Harris WA. Binocular impulse blockade prevents the formation of ocular dominance columns in cat visual cortex. *J Neurosci*. 1986;6(8):2117–2133.
29. Rangaswamy NV, Frishman LJ, Dorotheo EU, Schiffman JS, Bahrani HM, Tang RA. Photopic ERGs in patients with optic neuropathies: comparison with primate ERGs after pharmacologic blockade of inner retina. *Invest Ophthalmol Vis Sci*. 2004;45(10):3827–3837.
30. Viswanathan S, Frishman LJ, Robson JG, Harwerth RS, Smith EL. The photopic negative response of the macaque electroretinogram: reduction by experimental glaucoma. *Invest Ophthalmol Vis Sci*. 1999;40(6):1124–1136.
31. Fong MF, Duffy KR, Leet MP, Candler CT, Bear MF. Correction of amblyopia in cats and mice after the critical period. *Elife*. 2021;10:e70023.
32. Duffy KR, Bear MF, Patel NB, Das VE, Tychsen L. Human deprivation amblyopia: treatment insights from animal models. *Front Neurosci*. 2023;17:1249466.
33. Uhlrich DJ, Essock EA, Lehmkuhle S. Cross-species correspondence of spatial contrast sensitivity functions. *Behav Brain Res*. 1981;2(3):291–299.
34. Meier K, Giaschi D. Unilateral amblyopia affects two eyes: fellow eye deficits in amblyopia. *Invest Ophthalmol Vis Sci*. 2017;58(3):1779–1800.
35. Thompson B, Concetta Morrone M, Bex P, Lozama A, Sabel BA. Harnessing brain plasticity to improve binocular vision in amblyopia: an evidence-based update. *Eur J Ophthalmol*. 2024;34(4):901–912.
36. Kiorpes L. Understanding the development of amblyopia using macaque monkey models. *Proc Natl Acad Sci USA*. 2019;116(52):26217–26223.
37. Wensveen JM, Smith EL, 3rd, Hung LF, Harwerth RS. Brief daily periods of unrestricted vision preserve stereopsis in strabismus. *Invest Ophthalmol Vis Sci*. 2011;52(7):4872–4879.
38. Harwerth RS, Crawford ML, Smith EL, 3rd, Boltz RL. Behavioral studies of stimulus deprivation amblyopia in monkeys. *Vision Res*. 1981;21(6):779–789.
39. Brainard DH. The Psychophysics Toolbox. *Spat Vis*. 1997;10(4):433–436.
40. Norcia AM, Appelbaum LG, Ales JM, Cottereau BR, Rossion B. The steady-state visual evoked potential in vision research: a review. *J Vis*. 2015;15(6):4.
41. Snyder EW, Beck EC, Dustman RE. Visual evoked potentials in monkeys. *Electroencephalogr Clin Neurophysiol*. 1979;47(4):430–440.
42. Yildirim C, Tychsen L. Effect of infantile strabismus on visuomotor development in the squirrel monkey (Saimiri sciureus): optokinetic nystagmus, motion VEP and spatial sweep VEP. *Strabismus*. 1999;7(4):211–219.
43. Gavornik JP, Bear MF. The visual evoked potential is a sensitive and powerful measure of experience-dependent visual cortical plasticity in mice. *Curr Opin Neurobiol*. 2025;93:103019.
44. Hood DC, Frishman LJ, Viswanathan S, Robson JG, Ahmed J. Evidence for a ganglion cell contribution to the primate electroretinogram (ERG): effects of TTX on the multifocal ERG in macaque. *Vis Neurosci*. 1999;16(3):411–416.
45. Patel NB, Wheat JL, Rodriguez A, Tran V, Harwerth RS. Agreement between retinal nerve fiber layer measures from Spectralis and Cirrus spectral domain OCT. *Optom Vis Sci*. 2012;89(5):E652–E666.
46. Frishman LJ, Wang MH. Electroretinogram of human, monkey and mouse. *Adlers Physiol Eye*. 2011;24:480–501.
47. Robson AG, Frishman LJ, Grigg J, et al. ISCEV Standard for full-field clinical electroretinography (2022 update). *Doc Ophthalmol*. 2022;144(3):165–177.
48. Frishman L, Sustar M, Kremers J, et al. ISCEV extended protocol for the photopic negative response (PhNR) of the full-field electroretinogram. *Doc Ophthalmol*. 2018;136(3):207–211.

Investigative Ophthalmology & Visual Science

49. Bankhead P, Loughrey MB, Fernandez JA, et al. QuPath: open source software for digital pathology image analysis. *Sci Rep*. 2017;7(1):16878.
50. Yu W, Cao G, Qiu J, et al. Evaluation of monkey intraocular pressure by rebound tonometer. *Mol Vis*. 2009;15:2196–2201.
51. Budenz DL, Fredette MJ, Feuer WJ, Anderson DR. Reproducibility of peripapillary retinal nerve fiber thickness measurements with stratus OCT in glaucomatous eyes. *Ophthalmology*. 2008;115(4):661–666.e664.
52. Mwanza JC, Oakley JD, Budenz DL, Chang RT, Knight OJ, Feuer WJ. Macular ganglion cell-inner plexiform layer: automated detection and thickness reproducibility with spectral domain-optical coherence tomography in glaucoma. *Invest Ophthalmol Vis Sci*. 2011;52(11):8323–8329.
53. Patel NB, Lim M, Gajjar A, Evans KB, Harwerth RS. Age-associated changes in the retinal nerve fiber layer and optic nerve head. *Invest Ophthalmol Vis Sci*. 2014;55(8):5134–5143.
54. Srinivasan VV, Das S, Patel N. Widefield OCT imaging for quantifying inner retinal thickness in the nonhuman primate. *Transl Vis Sci Technol*. 2022;11(8):12.
55. Fortune B, Burgoyne CF, Cull GA, Reynaud J, Wang L. Structural and functional abnormalities of retinal ganglion cells measured in vivo at the onset of optic nerve head surface change in experimental glaucoma. *Invest Ophthalmol Vis Sci*. 2012;53(7):3939–3950.
56. Fortune B, Bui BV, Cull G, Wang L, Cioffi GA. Inter-ocular and inter-session reliability of the electroretinogram photopic negative response (PhNR) in non-human primates. *Exp Eye Res*. 2004;78(1):83–93.
57. Cohen CJ, Bean BP, Colatsky TJ, Tsien RW. Tetrodotoxin block of sodium channels in rabbit Purkinje fibers. Interactions between toxin binding and channel gating. *J Gen Physiol*. 1981;78(4):383–411.
58. Antwi-Boasiako K, Carter-Dawson L, Harwerth R, Gondo M, Patel N. The relationship between macula retinal ganglion cell density and visual function in the nonhuman primate. *Invest Ophthalmol Vis Sci*. 2021;62(1):5.
59. Kim CB, Tom BW, Spear PD. Effects of aging on the densities, numbers, and sizes of retinal ganglion cells in rhesus monkey. *Neurobiol Aging*. 1996;17(3):431–438.
60. Smith DW, Lee CJ, Gardiner BS. No flow through the vitreous humor: how strong is the evidence? [published online ahead of print February 6, 2020] *Prog Retin Eye Res*. doi:10.1016/j.preteyeres.2020.100845.
61. Bouskila J, Javadi P, Palmour RM, Bouchard JF, Ptito M. Standardized full-field electroretinography in the Green Monkey (Chlorocebus sabaeus). *PLoS One*. 2014;9(10):e111569.
62. Herbin M, Boire D, Ptito M. Size and distribution of retinal ganglion cells in the St. Kitts green monkey (Cercopithecus aethiops sabeus). *J Comp Neurol*. 1997;383(4):459–472.
63. Wong RO. Retinal waves and visual system development. *Annu Rev Neurosci*. 1999;22:29–47.
64. Moody WJ, Bosma MM. Ion channel development, spontaneous activity, and activity-dependent development in nerve and muscle cells. *Physiol Rev*. 2005;85(3):883–941.
65. Wollner DA, Scheinman R, Catterall WA. Sodium channel expression and assembly during development of retinal ganglion cells. *Neuron*. 1988;1(8):727–737.
66. Le Goff MM, Bishop PN. Adult vitreous structure and postnatal changes. *Eye (Lond)*. 2008;22(10):1214–1222.
67. Denlinger JL, Eisner G, Balazs EA. Age-related changes in the vitreus and lens of rhesus monkeys (Macaca mulatta). *Exp Eye Res*. 1980;31(1):67–79.
68. Wong-Riley M, Riley DA. The effect of impulse blockage on cytochrome oxidase activity in the cat visual system. *Brain Res*. 1983;261(2):185–193.
69. Wong-Riley M, Carroll EW. Effect of impulse blockage on cytochrome oxidase activity in monkey visual system. *Nature*. 1984;307(5948):262–264.
70. Wong-Riley MT, Norton TT. Histochemical localization of cytochrome oxidase activity in the visual system of the tree shrew: normal patterns and the effect of retinal impulse blockage. *J Comp Neurol*. 1988;272(4):562–578.
71. DiCostanzo NR, Crowder NA, Kamermans BA, Duffy KR. Retinal and optic nerve integrity following monocular inactivation for the treatment of amblyopia. *Front Syst Neurosci*. 2020;14:32.
72. Hagen NA, Cantin L, Constant J, et al. Tetrodotoxin for moderate to severe cancer-related pain: a multicentre, randomized, double-blind, placebo-controlled, parallel-design trial. *Pain Res Manag*. 2017;2017:7212713.
73. Singh R, Davoudi S, Ness S. Preventive factors, diagnosis, and management of injection-related endophthalmitis: a literature review. *Graefes Arch Clin Exp Ophthalmol*. 2022;260(8):2399–2416.
74. Phan C, Qiu M, Zhang AY. The association between intravitreal injections and glaucoma: an update. *Curr Opin Ophthalmol*. 2026;37(2):124–130.

Investigative Ophthalmology & Visual Science